NeuroImage: Clinical 25 (2020) 102197

Contents lists available at ScienceDirect

NeuroImage: Clinical

journal homepage: www.elsevier.com/locate/ynicl

Ventral stream hierarchy underlying perceptual organization in adolescents with autism

Laurie-Anne Sapey-Triomphe[a,b,#], Bart Boets[b,c,#,*], Lien Van Eylen[b,d], Ilse Noens[b,d], Stefan Sunaert[e], Jean Steyaert[b,c], Johan Wagemans[a,b]

[a] Laboratory of Experimental Psychology, Department of Brain and Cognition, Leuven Brain Institute, KU Leuven, Leuven 3000, Belgium
[b] Leuven Autism Research (LAuRes), KU Leuven, Leuven 3000, Belgium
[c] Center for Developmental Psychiatry, Department of Neurosciences, KU Leuven, Kapucijnenvoer 7h, PB 7001, Leuven 3000, Belgium
[d] Parenting and Special Education Research Unit, KU Leuven, Leuven 3000, Belgium
[e] Translational MRI, KU Leuven, Leuven 3000, Belgium

ARTICLE INFO

Keywords:
Autism spectrum disorder
Ventral visual stream
Object perception
fMRI, top-down processing

ABSTRACT

Object recognition relies on a hierarchically organized ventral visual stream, with both bottom-up and top-down processes. Here, we aimed at investigating the neural underpinnings of perceptual organization along the ventral visual stream in Autism Spectrum Disorders (ASD), and at determining whether this would be associated with decreased top-down processing in ASD. Nineteen typically developing (TD) adolescents and sixteen adolescents with ASD participated in an fMRI study where they had to detect visual objects. Five conditions displayed Gabor patterns (defined by texture and/or contour) with increasing levels of perceptual organization. In each condition, both groups showed similar abilities. In line with the expected cortical hierarchy, brain activity patterns revealed a progressive involvement of regions, from low-level occipital regions to higher-level frontal regions, when stimuli became more and more organized. The brain patterns were generally similar in both groups, but the ASD group showed greater activation than TD participants in the middle occipital gyrus and lateral occipital complex when perceiving fully organized everyday objects. Effective connectivity analyses suggested that top-down functional connections between the lower levels of the cortical hierarchy were less influenced by the meaning carried by the stimuli in the ASD group than in the TD group. We hypothesize that adolescents with ASD may have been less influenced by top-down processing when perceiving recognizable objects.

1. Introduction

We are constantly surrounded by objects that need to be segmented from their background, visually processed and identified, in order to understand our environment and to determine the possible interactions with it. Humans use several cues to detect objects and perform extremely well at visually identifying objects. The grouping of elementary features, based on cues such as proximity, orientation, similarity or collinearity, enables segmenting stimuli from noise, detecting shapes, and eventually recognizing objects. It has been well established that visual object recognition is accomplished in a series of processing steps throughout a hierarchically organized ventral visual stream. Several levels of abstraction of the visual information are provided through this neural hierarchy (Grill-Spector and Weiner, 2014; Wilson and Wilkinson, 2015). Low-level features of objects are processed posteriorly in the occipital cortex (e.g., contour orientation in V1), while higher-level properties such as global shape and object representations, are processed more anteriorly, along the ventral temporal cortex (Grill-Spector and Weiner, 2014). In particular, the lateral occipital complex (LOC) plays a major role in object perception (Haxby et al., 2001; James et al., 2003; Kim et al., 2009). This object-sensitive region is functionally characterized by a higher activation level for intact objects than for scrambled counterparts (Malach et al., 1995). Finally, conceptual processing of objects involves anterior regions, such as the anterior temporal pole and the orbitofrontal cortex (Bar, 2004; Sewards and Sewards, 2002).

It is important to emphasize the interactive and bidirectional nature of the ventral visual stream, involving not only bottom-up but also top-down processing streams between these brain regions (Ahissar and Hochstein, 2004; Clark, 2013; Mijović et al., 2014; Van Essen et al.,

* Corresponding author.
E-mail address: bart.boets@kuleuven.be (B. Boets).
Joint first authors

https://doi.org/10.1016/j.nicl.2020.102197
Received 24 July 2019; Received in revised form 22 January 2020; Accepted 24 January 2020
Available online 25 January 2020
2213-1582/ © 2020 The Authors. Published by Elsevier Inc. This is an open access article under the CC BY-NC-ND license (http://creativecommons.org/licenses/BY-NC-ND/4.0/).

1992). Top-down signals sent from higher-level areas contribute to disambiguate the incoming visual information and to optimize processing in lower-level regions (Friston, 2003; Murray et al., 2002; Rao and Ballard, 1999). A consequence of these top-down signals is a decrease in activation levels in low-level areas, as if the more local, lower-level activations are "explained away" by more global, higher-level interpretations (e.g., Kok et al., 2012). Top-down processing from frontal regions, such as the orbitofrontal cortex and the inferior frontal gyrus (Bar, 2007, 2004; Bar et al., 2006; Mulder et al., 2012; Sherman et al., 2016), would carry prior knowledge (i.e., predictions) about the object. Bar and colleagues, in particular, have shown that low-spatial frequency visual information quickly triggers predictions hosted in the left orbitofrontal cortex, which are subsequently fed back to verify whether they match the gradually assembled bottom-up information in the ventral visual stream (Bar, 2007, 2004; Bar et al., 2006). Importantly, this interactive interplay and flexible shift between bottom-up and top-down processes along the ventral visual stream constitute the basis of the amazing ability to rapidly capture the conceptual gist of a scene.

In Autism Spectrum Disorder (ASD), visual perception is often characterized as atypical and the interplay between these bottom-up and top-down processes may be altered. ASD refers to a spectrum of early onset neurodevelopmental disorders characterized by impairments in social interactions and communication, combined with repetitive and restricted patterns of behaviors and interests (DSM-5, American Psychiatric Association, 2013). Many theories of ASD have targeted increased focus on details and difficulties getting the "global picture" in ASD, because of an atypical balance characterized by enhanced low-level bottom-up processing and decreased top-down processing. The Enhanced Perceptual Functioning theory (Mottron et al., 2006; Mottron and Burack, 2001) has emphasized the idea of superior abilities for local processing in ASD, while the Weak Central Coherence theory (Frith, 1989; Happé and Frith, 2006) suggested reduced global processing in ASD leading to difficulties integrating sensory information into a meaningful whole. Yet, note that a recent meta-analysis did not reveal any increased local and decreased global visual processing biases in ASD, but simply a slower global visual processing in ASD (Van der Hallen et al., 2015).

More recent theories of ASD were formulated within the predictive coding framework to account for the atypical sensory perception in ASD. Some of these theories propose a reduced influence of top-down knowledge in ASD, because priors would have a lower precision than sensory inputs (Brock, 2012; Lawson et al., 2014; Pellicano and Burr, 2012). An alternative account is that prediction errors (i.e., mismatch between prior expectations and sensory inputs) would be characterized by a high and inflexible precision at the lower levels of the cortical hierarchy (Van de Cruys et al., 2014). Most of the theories of ASD predict that the visual processing of objects would be atypical in ASD. Especially, people with ASD would show decreased top-down processing when they perceive objects that need to be identified. This would be associated with increased activity in low-level regions of the ventral stream hierarchy and with decreased functional connections from higher-level to lower-level regions along the ventral visual stream. Interestingly, Hadjikhani and colleagues found typical organization of early visual areas in individuals with ASD and suggested that the peculiar visual processing encountered in ASD would result from atypicalities in higher-level regions and/or top-down processes (Hadjikhani et al., 2004).

In ASD, the ventral visual stream has been mostly investigated in studies focused on face perception. Such studies usually showed hypoactivations in face-related areas and higher activity in more object-related regions (Critchley et al., 2000; Hubl et al., 2003; Pierce et al., 2001; Scherf et al., 2010; Schultz et al., 2000). It is not clearly determined whether there is a specific disruption of face-related regions along the ventral visual pathway in ASD (Scherf et al., 2010). The ventral visual stream seems to be organized differently in ASD, with clear differences for face-selective regions, and more subtle differences for object perception. For instance, object perception has been associated with an increased variance of the BOLD signal in ASD (Humphreys et al., 2008), with a decreased object-related activation in the precuneus in ASD (Scherf et al., 2014) or with subtle differences in visual potentials evoked by contour or texture-defined shapes in children with ASD compared to typically developing children (Pei et al., 2009). In visuospatial tasks, such as the Embedded Figure Test, individuals with ASD showed increased activation in right ventral occipitotemporal regions, as compared to controls (Malisza et al., 2011; Ring et al., 1999). Contrary to many studies contrasting objects to faces or to scrambled images, the experimental design of the present study enables investigating the neural correlates of object perception for stimuli presenting with different levels of perceptual organization.

The present study aimed at precisely mapping out the neural regions along the ventral visual stream that underlie perceptual organization in adolescents with and without ASD. In addition, this study aimed at determining whether people with ASD show decreased top-down influence during visual perception of objects. We used functional MRI and a task showing Gabor patterns with different levels of organization, in order to characterize the involvement of brain regions along the ventral visual stream. An advantage of using Gabor elements is that they match the receptive fields of neurons in the primary visual cortex and they can also recruit higher-level regions when they become organized to depict objects. Indeed, depending on their differential orientations, Gabor elements can form shapes that can be recognizable, based on contour or texture features (Casco et al., 2009; Machilsen and Wagemans, 2011; Mijović et al., 2014; Sassi et al., 2012, 2010). After processing the Gabor elements and perceptually grouping them into a coherent shape in the lower levels of the visual hierarchy, top-down matching processes from higher-level areas will occur, especially for identifiable stimuli (Panis and Wagemans, 2009). According to the predictive coding framework, top-down signals would contribute to facilitate visual processing of objects in lower-level regions. In the present study, Gabor patterns were either randomly oriented or organized so that a shape, embedded in a background of randomly oriented Gabor elements, could be identified by its contour and/or texture. These stimuli depicted recognizable (i.e., meaningful) or non-recognizable objects (i.e., meaningless). Adolescents with and without ASD participated in an fMRI study where they had to detect the presence of organized patterns, appearing dynamically on a screen. Such task requires a dynamic interplay between bottom-up and top-down processes, as individual Gabor elements need to be grouped gradually, while prior knowledge about object representations needs to be matched to this incoming sensory input (Evers et al., 2014).

Previous studies showed that such stimuli, depicted by contour and/or texture and displaying meaningful or meaningless stimuli, could be detected by control participants (Sassi et al., 2012). A local bias towards individual Gabor patches would be associated with longer response times to detect shapes (Van der Hallen et al., 2015). According to theories such as the Weak Central Coherence theory (Frith, 1989; Happé and Frith, 2006), such a behavioral response could be expected in the ASD group. At the neural level, we should observe an involvement of low-level occipital regions when stimuli present with no (or little) organization. We expect a progressive involvement of higher-level occipital and frontal regions when stimuli get more organized and depict recognizable objects. We expect these regions to be revealed in a whole-brain analysis investigating the main effect of the experimental conditions. In addition, we will perform region of interest (ROI) analyses in regions along the ventral visual stream (V1, V2, V3, V4 and LOC) and in frontal regions (right IFG and left OFC) to demonstrate their involvement in each of the conditions (which display different levels of perceptual organization). Recognizable stimuli should elicit top-down signaling from high-level to lower-level regions along the ventral stream hierarchy. Besides, if the hierarchical processing of objects is altered in ASD, an atypical involvement of brain regions along

Table 1
Characteristics of the Typically Developing adolescents (TD group) and adolescents with Autism Spectrum Disorder (ASD group).

		TD group	ASD group	*p-value*
Number of participants		19	16	–
Male / Female number		19 / 0	19 / 0	–
Age (years)		14.1 (± 2.1)	13.9 (± 1.8)	*ns*
Left-handed / Right-handed		2 / 17	2 / 14	*ns*
Intellectual Quotient (IQ):	*Performance IQ*	111 (± 15)	99 (± 17)	.05
	Verbal IQ	116 (± 13)	101 (± 20)	.02
	Total IQ	114 (± 10)	100 (± 16)	< 0.01
Social Responsiveness Scale:	*Total score*	43 (± 5)	92 (± 6)	< 0.001

The table presents the group means (± standard deviations) and p-values of the Student t-tests performed between groups.

the ventral stream hierarchy would be expected. More specifically, a decreased top-down processing in ASD would be associated with greater activation levels in low-level regions of the ventral stream, such as V1 or V2 (according to the "explaining away hypothesis"). It would also be associated with decreased top-down functional connections along the ventral stream hierarchy in ASD, when perceiving recognizable objects. Prior knowledge elicited by recognizable stimuli should be associated with brain responses in frontal regions, such as the inferior frontal gyrus and the orbitofrontal cortex, which could be atypical in the ASD group.

2. Materials and methods

2.1. Participants

Twenty typically developing (TD) adolescents and 19 adolescents with ASD participated in the fMRI study. One TD adolescent and three adolescents with ASD were discarded from the analyses due to excessive movements during fMRI acquisition. The demographic characteristics of the participants (19 TD and 16 ASD participants) are described in Table 1. Inclusion criteria were having a full-scale intellectual quotient above 80 and having normal or corrected-to-normal vision. Exclusion criteria were having epilepsy, traumatic brain injury, attention deficit/hyperactivity disorder, or any contraindications to participate in an MRI study. In addition, TD adolescents were excluded if they had a history of neurological or psychiatric conditions, or a current medical, developmental or psychiatric diagnosis. For ASD participants, additional exclusion criterion was having ASD associated with an identified genetic syndrome. None of the participants reported taking psychotropic medication at the time of the experiment.

Participants with ASD received their diagnosis from a multidisciplinary Expertise Centre for Autism (University Hospitals KU Leuven), in a standardized way according to DSM-IV-TR criteria (American Psychiatric Association, 2000). Furthermore, their diagnosis was confirmed with the Developmental, Dimensional and Diagnostic interview (Skuse et al., 2004) and with the Social Responsiveness Scale (SRS) (Roeyers et al., 2013, 2011) where T-scores were above 65. In order to exclude the presence of substantial ASD characteristics, parents of the TD adolescents also completed the SRS questionnaire (Table 1).

The study was approved by the Medical Ethical Committee of the University Hospital Leuven. An informed consent was obtained from all parents according to the Declaration of Helsinki, with additional assent from all participating adolescents.

2.2. Stimuli

Visual stimuli consisted of Gabor patches displayed on a uniform grey background. These visual patterns encompassed on average 2056 Gabor elements (11.5 × 11.5° visual angle) and were projected on a high-resolution computer screen at the end of the scanner cylinder. Stimuli were created using the Grouping Elements Rendering Toolbox (Demeyer and Machilsen, 2012). Note that these stimuli are well controlled and have been quite extensively used in previous experiments (e.g., Evers et al., 2014; Sassi et al., 2012, 2010). The Gabor patterns dynamically evolved from a random orientation to a final orientation, within 5400 ms (following 12 logarithmic steps, including eleven 355 ms frames and one 1495 ms end frame). There were five different conditions presenting different levels of organization in the final orientation of the Gabor patches: one *Random* condition and four organized conditions (Fig. 1). Across the four organized conditions, stimuli were matched for average number of Gabor elements on the contour, in the figure and in the background, and for average compactness of the figure. Videos showing examples of the *Random* condition and of the four organized conditions are available as supplementary materials.

In the *Random* condition, the Gabor patches of the stimuli evolved into another random orientation. In the *Contour* condition, stimuli evolved into contour-defined non-existent objects: outline Gabor patches reoriented curvilinear to the outline of an object, while interior and exterior Gabor patches reoriented to a random position. In the *Texture* condition, stimuli evolved into a texture-defined non-existent object: interior Gabor patches reoriented parallel to the main axis of an object, while exterior Gabor patches reoriented to a position orthogonal to this. In the *Contour & Texture Meaningless* condition, stimuli evolved into non-existent objects that were defined by contour and texture. Finally, in the *Contour & Texture Meaningful* condition, stimuli evolved into everyday objects that were defined by contour and texture. In the *Contour & Texture* conditions (*Meaningful* and *Meaningless*), interior Gabor patches reoriented parallel to the main axis and outline Gabor patches reoriented curvilinear to the outline of an object. In the *Contour & Texture Meaningful* condition, everyday objects were selected from the Snodgrass and Vanderwart stimulus set (Snodgrass and Vanderwart, 1980). Only stimuli with a very high recognition rate in typically developing adults were selected as everyday objects (i.e. 100% correct recognition on the basis of the combination of Contour & Texture, and over 95% on the basis of texture or contour solely; see Sassi et al., 2010).

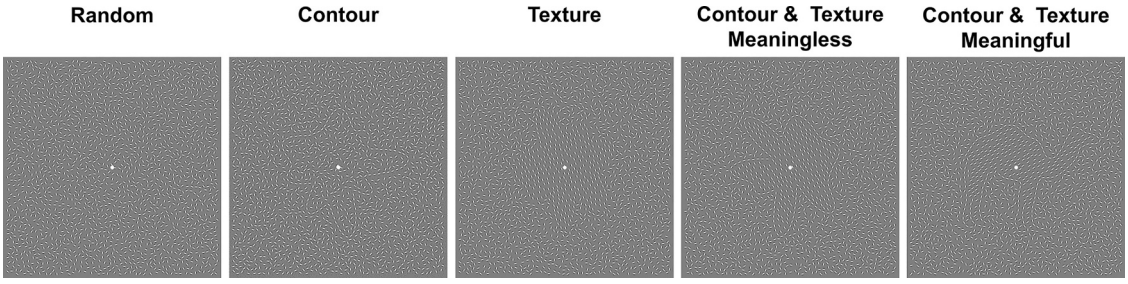

Fig. 1. Examples of stimuli
Gabor patches dynamically evolved from a random orientation to another orientation within 5400 ms. Videos showing examples of stimuli are available as supplementary materials.

2.3. Experimental paradigm

Each experimental trial consisted of a stimulus presented for 5400 ms, followed by a grey screen displayed for 600 ms. Participants were instructed to fixate a white dot located in the center of the screen, and to press the button as soon as they detected a figure or pattern on the screen. Baseline trials consisted of a grey screen displayed for 6000 ms.

Participants performed two event-related fMRI runs. Each fMRI run consisted of 67 trials: 10 presentations of each of the five conditions (*Random, Contour, Texture, Contour & Texture Meaningless, Contour & Texture Meaningful*) and 17 fixation trials (baseline). Total scan duration was 402 s per run. Trial order was optimally counterbalanced by means of a genetic algorithm (Wager and Nichols, 2003).

Stimulus presentation and response registration were controlled by Eprime 1.1 software (Psychology Software Tools, Pittsburgh, PA).

2.4. MRI data acquisition

Participants were first familiarized with a mock scanner, before being installed in the MR scanner. Functional and structural brain scans were acquired on a 32 head coil 3T Philips Achieva system at the University Hospital of Leuven (UZ Leuven).

A high-resolution T1-weighted anatomical scan was collected (182 contiguous coronal slices, voxel size = 0.98 × 0.98 × 1.2 mm^3, TR = 9.6 ms, TE = 4.6 ms, FOV = 250 × 250 × 218 mm^3, acquisition matrix = 256 × 256, acquisition time = 6 min 23 s).

Whole-brain T2*-weighted echo-planar imaging sequences were acquired (voxel size = 3.0 × 3.0 × 3.5 mm^3, TR = 2 s, TE = 30 ms, flip angle = 90°, FOV = 220 × 220 × 133 mm^3, 37 contiguous ascending slices), using blood-oxygenation-level dependent (BOLD) imaging. In each functional run, 201 functional volumes were acquired.

2.5. MRI preprocessing

Functional MRI data were preprocessed using the CONN functional connectivity SPM toolbox 2017 (Whitfield-Gabrieli and Nieto-Castanon, 2012) (http://www.nitrc.org/projects/conn), within Matlab 2017b. Preprocessing consisted of realignment of the functional volumes, slice timing correction with the first slice as reference, outlier detection using the ART Artifact Detection toolbox (https://www.nitrc.org/projects/artifact_detect/) with a motion threshold of 2 mm, coregistration on the anatomical T1 scan, segmentation and normalization. The template image for spatial normalization was based on the standard template of the Montreal Neurological Institute (MNI). Finally, normalized images were smoothed with a Gaussian smoothing kernel of 8 mm (full width at half maximum).

Unique regressors were used to discard the ART-based identified outlier scans from the analysis. Motion parameters were also modelled as separate regressors.

In addition, within the CONN toolbox, we performed a denoising step in order to remove physiological confounds from the signal (Behzadi et al., 2007). This step consisted of a principal component analysis on the cerebrospinal fluid and white matter masks using aCompCor (Behzadi et al., 2007). Results of the 10 first principal components were added as separate regressors to the General Linear Model (GLM) design matrix.

2.6. Functional MRI analyses

We defined a GLM using six main regressors: a baseline regressor (6-second long, during grey displays), and a regressor for each of the five stimulus categories. Event-timing of correct object detection in the organized conditions was time-locked to individual response times. Event-timing for the *Random* condition was fixed at 1 s post-stimulus onset. False alarms in the *Random* condition and unanswered trials in the four types of organized conditions were removed from the analyses. The six movement parameters, the ART-based outlier scans, and the principal components of the denoising step were added to the GLM. Low-frequency drifts were removed using a temporal high-pass filter (cut-off, 128 s).

For each subject, contrast images were computed for the five conditions vs. baseline using *t*-statistics. We performed a factorial analysis investigating the factors groups (TD and ASD) and conditions (*Random, Contour, Texture, Contour & Texture Meaningless, Contour & Texture Meaningful*). In order to illustrate the results of the main effect of condition on brain activity, we performed the ROI analysis described in the following section.

For each condition and group, the mean of the contrasts across subjects was compared to zero using a one-sample Student's *t*-test. Brain patterns were compared between the two groups using independent two-sample t-tests. When there was a group difference, we used Marsbar (Brett et al., 2002, release 0.44) to extract the mean contrast estimate in the cluster showing a significant group difference ($p < .001$ at the voxel level, $p < .05$ at cluster level), and we plotted the distribution of contrast estimates across participants.

Statistical threshold was set at $p < .001$ at the voxel level and $p < .05$ at cluster level. We report whether these results remain significant after Family Wise Error (FWE) correction at cluster level.

2.7. Regions of interest (ROI) analyses

2.7.1. Choice of the ROIs

Based on the existing literature, we decided to focus on the following regions of interests (ROI): V1, V2, V3, V4, the bilateral lateral occipital complex (LOC), the left orbitofrontal cortex (OFC) and the right inferior frontal gyrus (IFG).

We decided to select V1, V2, V3, V4 and the LOC in order to include regions along the ventral visual stream, involved in object recognition and tuned for visual features of increasing complexity. As we did not have prior hypotheses about the lateralization of these regions, we included both left and right regions to define the ROI.

In addition, we included two frontal regions: the left OFC and the right IFG, as these brain regions may be involved in generating top-down contextual predictions. Throughout a series of studies, Bar and colleagues consistently demonstrated that left orbitofrontal cortex activity precedes object recognition related activity in temporal areas, and is driven by low spatial frequency and magnocellular-biased visual input (Bar et al., 2006; Chaumon et al., 2014; Kveraga et al., 2007). Besides, we decided to include the right IFG (triangular part) as it may play a role in generating precision-weighted top-down predictions (e.g., Sherman et al., 2016).

Note that the choice of the ROIs was hypothesis-driven, but that the definition of the coordinates of the ROIs was data-driven. As these coordinates were chosen based on the results of the whole-brain analyses (see Sections 2.7.2 and 2.7.3), these analyses are not meant to provide new results, but simply to illustrate more clearly the effect of conditions and group in a subset of ROIs.

2.7.2. Creation of the structural masks

We first created structural masks, by selecting the ROI defined in the Anatomy Toolbox (SPM12). For bilateral ROIs, left and right masks were merged into one ROI using Marsbar (Brett et al., 2002, release 0.44). V1 and V2 masks were also merged using Marsbar. For the left OFC, we selected the OFC-FO3 as defined in the Anatomy Toolbox, based on previous literature (Bar et al., 2006; Chaumon et al., 2014; Kveraga et al., 2007). For the right IFG, we selected the triangular part, as defined in the Anatomy Toolbox (Sherman et al., 2016). For the LOC, as we did not have any functional localizers and as the object-sensitive LOC is not determined by anatomic boundaries nor included in anatomic atlases, this ROI was defined by using fMRI data of another independent study comprising typically developing adults (Martens et al.,

2018). A second level "objects vs. scrambled objects" group contrast ($p < .05$, FWE corrected) resulted in a large region covering most of occipitotemporal and part of parietal cortex. Increasing the threshold to $t > 10$ combined with anatomical masking to inferotemporal cortex resulted in a bilateral spot that matched perfectly with the size and location of LOC as described in the literature (Grill-Spector et al., 1998; Vinberg and Grill-Spector, 2008), spanning the following MNI coordinates: lateral-medial $x = -46$ to -34 (left) and $x = 28$ to 48 (right), anterior-posterior $y = -34$ to -74 (left) and $y = -31$ to -61 (right), superior-inferior $z = -8$ to -22 (left) and $z = -8$ to -26 (right).

2.7.3. Extraction of the time-series

We displayed the main effect of condition on the fMRI results (two groups pooled together) and masked these results with the structural masks defined above. We then extracted the coordinates of the peak activity ($p < .001$) in each of the ROIs (see Supplementary Table 1). Using Marsbar, we created an 8 mm sphere around these coordinates and extracted the contrast estimate for each condition (random or organized conditions vs. baseline). We used these equally sized ROIs for the fMRI ROI analyses (Fig. 3) and for the functional connectivity analyses (Fig. 7).

2.7.4. ROI data analyses

We performed a nested ANOVA with the factor condition on the mean contrast estimate. We used Student t-tests as post-hoc analyses and we corrected for multiple comparisons using Holm-Bonferroni correction. Note that these ROI analyses were not performed in order to highlight new results, but to present the factorial analysis results in a more comprehensive way.

2.8. Functional connectivity analysis

Functional connectivity analyses were achieved using the CONN functional connectivity SPM toolbox 2017 (Whitfield-Gabrieli and Nieto-Castanon, 2012) within Matlab 2017b on data preprocessed and denoised, as described in the MRI data preprocessing section. We used the six ROIs described in the ROI section (V1-V2, V3, V4, LOC, OFC and IFG) and we performed ROI to ROI functional connectivity analyses within each group. Functional connectivity matrices were calculated by extracting the mean BOLD time series within each ROI per condition, and by correlating them with the time series of the other ROIs. We used two-sided pairwise t-tests with an alpha threshold set at 0.05. We applied the *FDR seed-level* correction of the CONN toolbox: for each ROI, the functional connections are FDR-corrected across five target regions.

2.9. Effective connectivity analysis

We used dynamic causal modelling (DCM, Friston et al., 2003) in order to investigate effective connectivity, as implemented in SPM12. Using DCM enables to make inferences about the causal relationships of activity patterns between brain regions, and so, to differentiate between feedforward and feedback functional connections (Friston et al., 2003). It also enables investigating modulation of functional connections by a factor present in certain stimuli, such as the fact that stimuli were sometimes presenting meaningful objects in the current study.

2.9.1. GLM definition

The GLM used to extract the time series for the DCM analyses was defined as follow. There were two main regressors, a *Visual input* regressor capturing the presentation of any visual stimuli (i.e., concatenation of the regressors described in the fMRI analyses section: *Random, Contour, Contour & Texture, Contour & Texture Meaningless, Contour & Texture Meaningful* regressors), and a *Meaning* regressor capturing the presentation of Meaningful stimuli (i.e., similar to the *Contour & Texture Meaningful* regressor described above). Like in the fMRI analysis, the motion parameters, the ART-based outlier scans and the principal components of the denoising step were added to the GLM. After running a first-level analysis with this GLM, we performed a second-level analysis using a factorial analysis with the factor group (two levels) and condition (two levels).

2.9.2. Time-series extraction

Time series were then extracted in three ROIs in the left hemisphere: inferior occipital gyrus (IOG), object-sensitive LOC and OFC. ROIs were defined based on anatomical and functional criteria. The general two-step procedure was the following: for each ROI, we first identified the maximum activity at the group level, before identifying the maximum activity at the individual level. This procedure was based on methods used in previous studies (Cardin et al., 2011). We first used the activity maxima at the group level for specific contrasts and anatomical masks to create a 25mm-diameter sphere around that maximum. These spheres were created using Marsbar. The group maximum for the IOG ROI ($x = -24, y = -87, z = -12$) was defined as the peak activity for the contrast *Visual input* vs. baseline (two groups combined), masked by the V1-V2 and V3 structural masks (described above). The group maximum for the LOC ROI ($x = -36, y = -48, z = -18$) was defined as the peak activity for the contrast *Meaning* vs. baseline (two groups combined), masked by the LOC structural mask (described above). Finally, the group maximum for the OFC ROI ($x = -33$, $y = 33$, $z = -12$) was defined as the peak activity for the contrast *Meaning* vs. baseline (two groups combined), masked by the OFC structural mask (described above). Then, within this 25mm-diameter sphere, we extracted the coordinates of the peak activity for similar contrasts of each individual participant (Supplementary Table 2). We extracted the first eigenvector across all voxels that were above the indicated peak threshold for the condition of interest, within a 6mm-radius sphere, centered on the maxima of each participant (Supplementary Table 2). We excluded two participants (one TD and one ASD) who showed no suprathreshold voxels in the OFC ROI. The mean size of the individual ROIs did not differ between groups (VOI sizes in voxels: IOG: 30 ± 6 [TD] and 30 ± 4 [ASD], LOC: 31 ± 3 [TD] and 32 ± 3 [ASD], OFC: 15 ± 7 [TD] and 15 ± 9 [ASD]).

2.9.3. DCM specification, estimation and comparison

We modelled as input all the visual stimuli displayed (*Visual input* regressor), entering the DCM through the IOG ROI. We specified one modulatory influence: the effect of meaning (*Meaning* regressor), modulating top-down functional connections from the OFC to the LOC and/or from the LOC to the IOG. We specified five models (Fig. 8A), two without modulation (models M1 and M2) and three with a modulatory influence of meaningful stimuli (models M3, M4 and M5). The models differed in terms of which functional connections were present and which were modulated by meaning. We considered a lower level of the cortical hierarchy (connections between the IOG and the LOC) and a higher level of the hierarchy (connections between the LOC and the OFC). In model M1, connections were only feedforward at the higher level of the cortical hierarchy, whereas these connections were both feedforward and feedback in M2, M3, M4 and M5. There was a modulatory influence of meaning on the low-level functional connections in M3, on the high-level functional connections in M4 and on the low and high-level connections in M5. For each participant, we estimated these five models separately. We used Bayesian model selection, in order to identify the model that best fitted our fMRI data, at the group level.

2.10. Statistical analyses

2.10.1. Behavioral data

Demographic data and neuropsychological assessments (Table 1) were compared between groups using Student t-tests. The mean percentage of correct detection and response times were analyzed using a repeated-measure ANOVA, with the factor group (TD and ASD) and

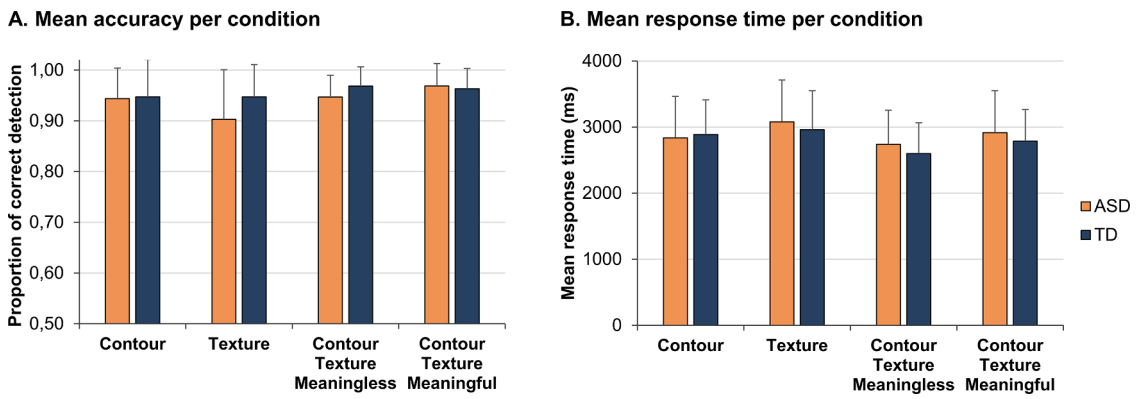

Fig. 2. Behavioral results
A. Mean accuracy (i.e., percentage of correct detection) per condition and group. **B.** Mean response time to detect a pattern or figure per condition and group. Error bars indicate standard deviations.

condition (five levels). Correlations between the intelligence quotient or the SRS score and the behavioural results were investigated using Pearson correlation tests. Statistical analyses were performed using R (version 2.15.3, http://www.r-project.org/). The threshold for statistical significance was set at $p < .05$.

2.10.2. MRI data

The statistical analyses of the fMRI analyses, ROI analyses, functional connectivity analyses and effective connectivity analyses are described above. They were all performed using Matlab 2017b. To label brain regions revealed during the MRI analyses, we used MARINA atlas (Walter et al., 2003) and the SPM Anatomy Toolbox including probabilistic cytoarchitectonic mapping (Eickhoff et al., 2005). To illustrate the brain activation patterns in Figs. 4 and 6, bspmview (version 20161108) was used (Spunt, 2016).

3. Results

3.1. Behavioral results

Both TD and ASD adolescents succeeded at detecting patterns in the four conditions presenting organized stimuli (mean percentage of correct detection superior to 90% in every group and condition). There were no significant effects of the factor group or condition and no interaction between group and condition on the percentage of correct detection, nor on the mean response time. The mean performance level and the mean response times for each group are shown in Fig. 2A and B, respectively. The response times indicate that on average, adolescents with and without ASD were able to detect figures presenting 83% of organization. These two variables were not significantly correlated with the SRS score in any group. Note that there was a tendency toward a positive correlation between the SRS score and the mean response time in the TD group only ($r = 0.40$, $p = .09$). These behavioral variables were not correlated with the intellectual quotient in neither group nor in the two groups combined.

3.2. Functional MRI results

3.2.1. Factorial analysis

3.2.1.1. Main results. There was a main condition effect on brain activity, mostly in the occipital cortex, posterior inferior temporal cortex, inferior, medial and precentral gyri of the frontal cortex, insula

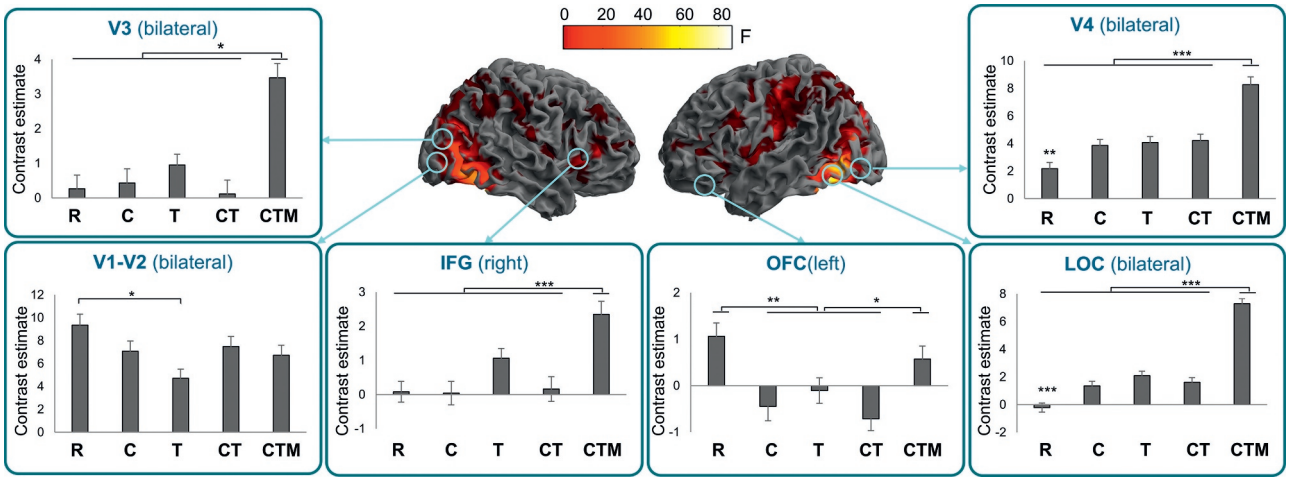

Fig. 3. Main effect of condition on brain activity and ROI analyses
The two groups are merged in this analysis (correction: $p < .001$ at peak level and $p < .05$ at cluster level). The histograms show the results of the ROI analyses for the conditions *Random* (R), *Contour* (C), *Texture* (T), *Contour & Texture Meaningless* (CT), and *Contour & Texture Meaningful* (CTM). Error bars indicate standard errors of the mean. * $p < .05$, ** $p < .01$, *** $p < .001$.

and anterior cingulate cortex (Fig. 3 and Supplementary Table 3). There was no main effect of group on brain activity.

There was an interaction between group and condition on brain activity in the right inferior/middle frontal gyri and in the left superior occipital cortex (Supplementary Table 3).

3.2.1.2. ROI analyses. In order to further illustrate the modulation of brain activity by condition, we performed ROI analyses in the brain regions showing a condition effect and where we had prior hypotheses. The ROI analyses are presented in the histograms of Fig. 3. As expected given the selection of the ROIs based on the factorial analysis results, the ANOVA performed on the mean contrast estimates in each ROIs showed a condition effect (F values ranging from 14 to 129, all $p < 10^{-6}$). Pairwise t-tests FDR-corrected were used as post-hoc tests.

Texture stimuli elicited less activity than *Random* stimuli ($p < .01$) in V1-V2. Displaying *Contour & Texture Meaningful* stimuli elicited more brain activity than any other kind of stimuli tested in V3 (all $p < 10^{-5}$), V4 (all $p < 10^{-8}$), the LOC (all $p < 10^{-8}$) and the right IFG (all $p < .05$). *Random* stimuli elicited less activity than every other type of organized stimuli in V4 (all $p < .05$) and the LOC (all $p < .001$). Finally, in the left OFC, *Random* stimuli elicited greater activity levels than *Contour, Texture, Contour & Texture Meaningless* (all $p < .01$), and *Contour & Texture Meaningful* stimuli elicited greater activity levels than *Contour* ($p < .05$) and *Contour & Texture Meaningless* ($p < .01$).

3.2.2. Brain activity patterns across the five conditions

3.2.2.1. Within-group analyses. The brain activity patterns associated with the five conditions vs. baseline are presented in Fig. 4 and in the Supplementary Table 4. There is a progressive involvement of brain regions, from low-level occipital regions to higher-level frontal regions when the stimuli become more organized and meaningful, as expected. In the TD and ASD groups, the patterns of brain activation across the five conditions were relatively similar (Fig. 4).

3.2.2.2. Between-group analyses. The TD and ASD groups differed in the contrast *Contour & Texture Meaningful* compared to baseline (Fig. 5). Indeed, the ASD group showed increased activity compared to the TD group in the middle occipital gyrus (left MOG: $x = -36$, $y = -78$, $z = -6$, size = 28, $T = 4.6$, right MOG: $x = 42$, $y = -81$, $z = 3$, size = 35, $T = 4.0$) and in the right object-sensitive LOC ($x = 33$, $y = -51$, $z = -18$, size = 34, $T = 5.3$).

In addition, there were two other marginal group differences (Fig. 1 of the Supplementary Material). The TD group showed increased activation compared to the ASD group in the left cuneus in the *Contour* condition (yet, note that the mean contrast estimate was not different from zero in the ASD group: $t(15) = 0.3$, $p > .05$) and in the left superior frontal gyrus in the *Texture* condition (yet, note that the mean contrast estimates was not different from zero in the TD group: $t(18) = 1.2$, $p > .05$).

In these brain clusters, the variance of the mean contrast estimates was larger in the ASD group than in the TD group (F-tests to compare variances: left cuneus: $p = 0.06$, left superior frontal gyrus: $p = .05$, left MOG: $p < 0.001$, right MOG: $p = .02$ and right LOC: $p = .01$).

Single-subject activation levels in these brain clusters were not

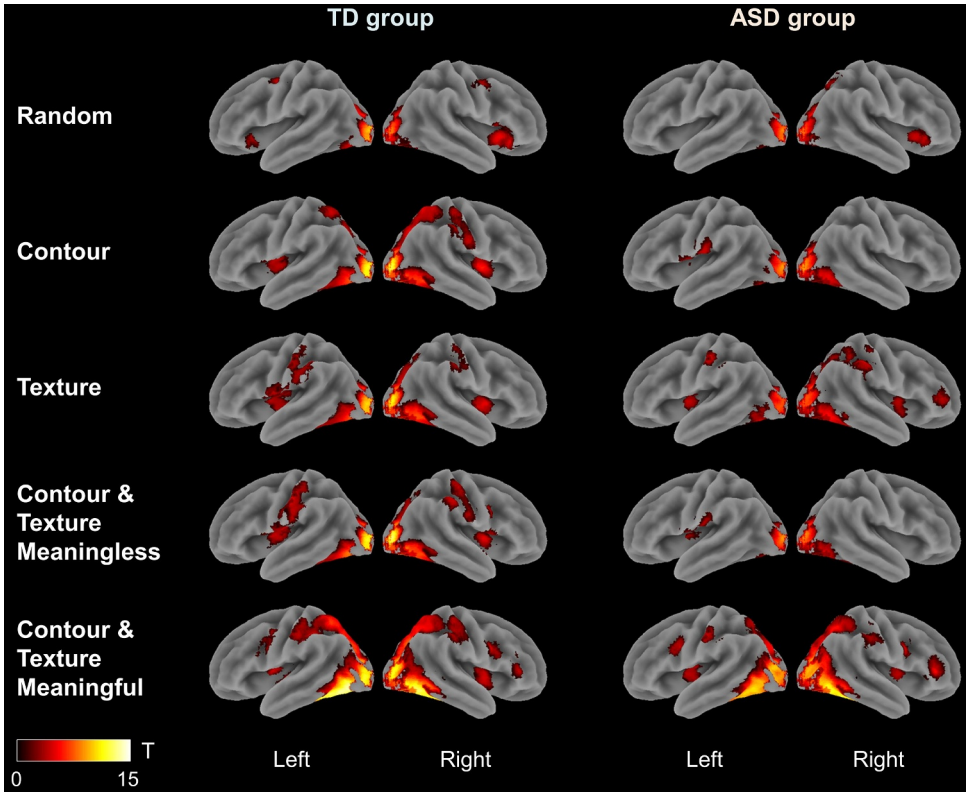

Fig. 4. Brain activity pattern per condition and group

Results of the contrasts condition vs. baseline (correction: $p < .001$ at peak level and $p < .05$ at cluster level). Cluster coordinates, sizes and p-values are provided in the Supplementary Table 4.

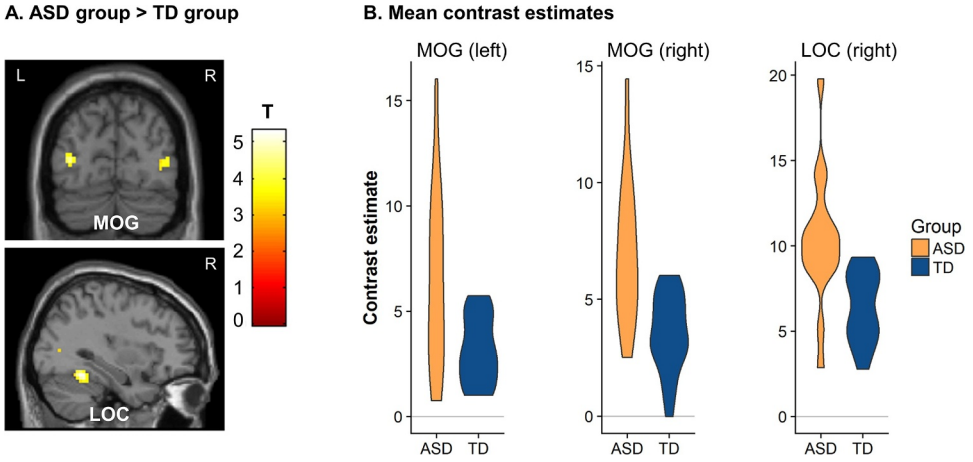

Fig. 5. Group differences in the condition *Contour & Texture Meaningful* vs. baseline
A. Illustration of the contrast ASD group > TD group, for the condition *Contour & Texture Meaningful* vs. baseline. Correction: $p < .001$ at voxel level and $p < .05$ at cluster level. **B.** Distribution of the mean contrast estimates in the ASD (orange) and TD (blue) groups, for the clusters shown in Fig. 5A. The mean contrast estimates are different from zero in both groups (one-sample t-tests, with t-values ranging from 6.2 to 13.8 and all p-values $< 10^{-4}$) and are significantly higher in the ASD group than in the TD group. LOC: lateral occipital complex; MOG: middle occipital gyrus.

significantly correlated with the intelligence quotient in any of the groups.

3.2.3. Contour & texture organized stimuli: meaningful vs. meaningless
3.2.3.1. Within-group analyses. We further investigated the contrast *Contour & Texture Meaningful* vs. *Meaningless* in order to identify brain clusters whose activity was increased when stimuli were recognizable (note that the level of perceptual organization is similar in the two conditions). The brain patterns were quite similar in each group (Fig. 6A) and mostly encompassed the bilateral LOC and the triangular and orbital parts of the inferior frontal gyrus (Supplementary Table 5).

3.2.3.2. Between-group analyses. For the contrast *Contour & Texture Meaningful* vs. *Meaningless*, the TD group did not show greater activity levels than the ASD group. Yet, compared to TD, the ASD group showed increased activity in the bilateral LOC and in the right IFG (Supplementary Table 5, Fig. 6B).

3.3. Connectivity results

3.3.1. Functional connectivity results

Functional connectivity analyses were performed in order to characterize the brain network involved in processing each type of stimuli (from random to more organized). Fig. 7 presents the results of the functional connectivity ROI to ROI analyses, between V1-V2, V3, V4, LOC, left OFC and right IFG in each group. Across the five conditions, from the less organized (*Random*) to the most organized and meaningful condition (*Contour & Texture Meaningful*), we can observe an increase in the network complexity. This increase in complexity is mostly due to more functional connections between the left OFC and the other brain regions (V1-V2, V3, V4, LOC and IFG). Group comparisons were performed in each condition and showed no significant group differences between patterns of functional connectivity (FDR-corrected).

3.3.2. Dynamic causal modelling results

We carried out a dynamic causal modelling analysis (DCM) in order

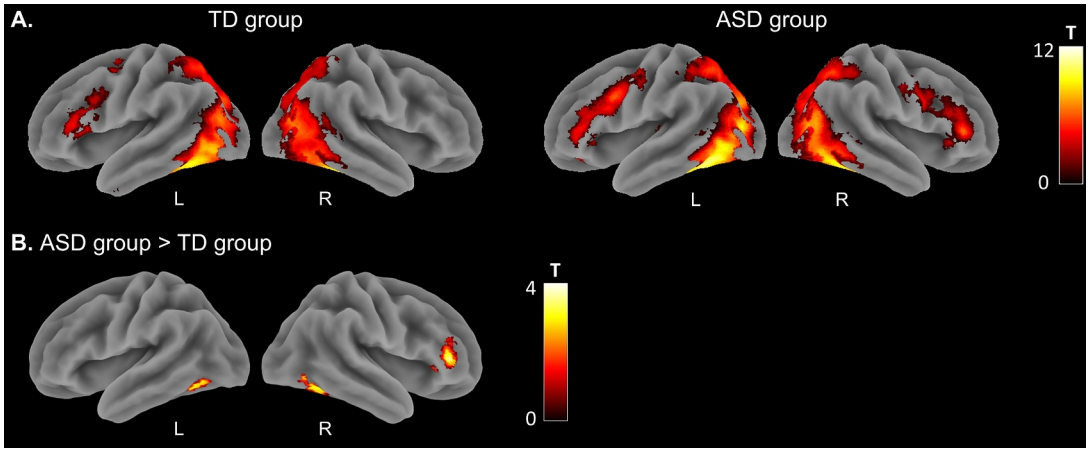

Fig. 6. Contrast *Contour & Texture Meaningful* vs. *Contour & Texture Meaningless*
A. Brain activity pattern per group. **B.** Group comparison: ASD group > TD group. Correction: $p < .001$ at the peak level and $p < .05$ at the cluster level. L: left, R: right.

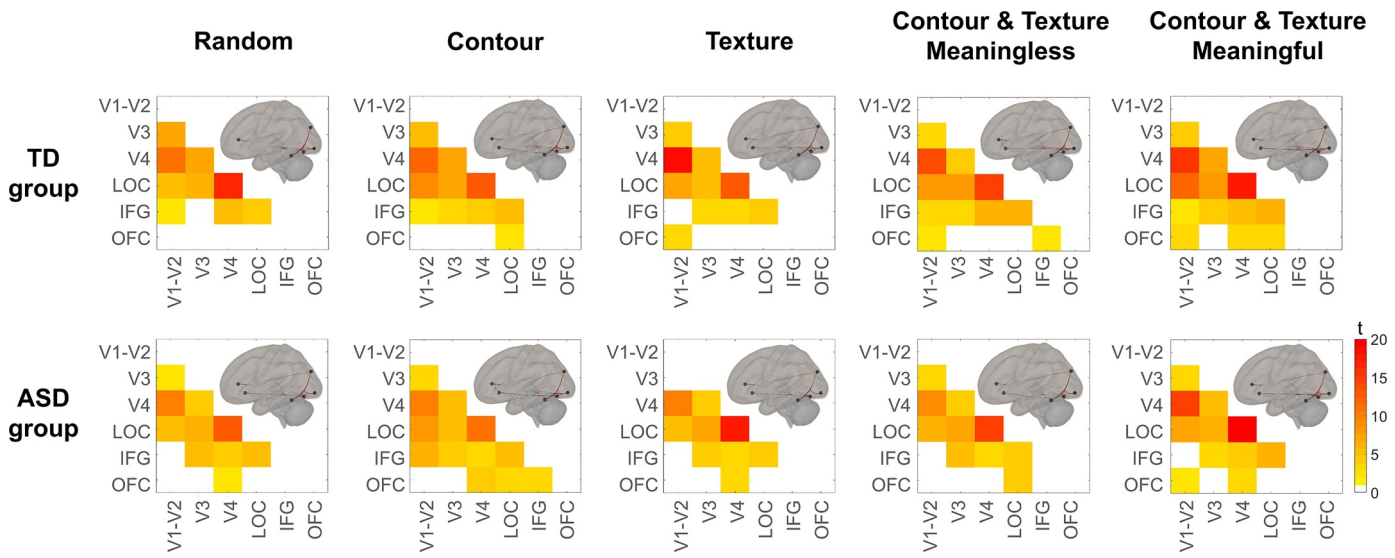

Fig. 7. Functional connectivity patterns per condition and group
ROI to ROI functional connectivity analyses were performed between V1-V2 bilateral, V3 bilateral, V4 bilateral, lateral occipital complex (LOC), left orbitofrontal cortex (OFC) and right inferior frontal gyrus (IFG). The figure shows results from two-sided pairwise t-tests with an alpha threshold set at 0.05 and FDR correction at the seed level. Yellow to red boxes indicate significant t-tests, while white boxes indicate non-significant t-tests.(For interpretation of the references to colour in this figure legend, the reader is referred to the web version of this article.)

to investigate whether individuals with ASD received less feedback from higher level regions and showed less or different top-down modulation when stimuli were meaningful. We compared five hierarchical models (Fig. 8A) and performed Bayesian model selection to identify the model that best fitted the fMRI data in each group. In the TD group (Fig. 8B), the model comparison revealed that Model 5 (M5) had the highest exceedance probability (M5: 0.55, M1 to M4: < 0.17, chance level: 0.20). M5 corresponds to the model including feedforward and feedback functional connections between the inferior occipital cortex (V1, V2 and surrounding cortex) and the object-sensitive LOC, and between the LOC and the orbitofrontal cortex, with feedback connections being modulated by the presence of meaningful stimuli. In the ASD group (Fig. 8B), the model comparison showed less conclusive results than in the TD group, with Model 4 showing the highest exceedance probability (M4: 0.41, M2 and M3: 0.21, M1 and M5 < 0.13, chance level: 0.20). Compared to Model 5, Model 4 does not include a modulation of feedback connections between the LOC and the inferior occipital cortex by meaningful stimuli.

4. Discussion

The main objective of the current study was to characterize the neural underpinnings of perceptual organization along the ventral visual stream in ASD. Especially, it aimed at identifying the neural networks involved in the visual perception of objects presenting with different levels of perceptual organization in adolescents with and without ASD. In addition, it investigated whether the neural mechanisms underlying perceptual grouping and object detection in ASD were characterized by reduced top-down modulation. At the behavioral level, TD and ASD adolescents showed similar abilities to detect shapes embedded in a background of randomly oriented Gabor elements. Whether the shapes were depicted by contour only, texture only or both contour and texture did not influence accuracy or response time in any group. Recognizable and unrecognizable objects did not lead to different behavioral responses either. The brain activity patterns associated with the visual detection of these shapes revealed a progressive involvement of brain regions, from low-level to higher-level areas along the ventral visual stream hierarchy, when the stimuli were getting more and more organized. The brain activation patterns did not show many differences in the ASD compared to the TD groups. Presenting meaningful stimuli (i.e., recognizable objects vs. baseline) was associated with greater activity in the LOC and middle occipital gyri in the ASD group than in the TD group. Displaying meaningful objects modulated top-down functional connections between regions of the ventral visual stream in both groups. Yet, this modulation was present both at the low and high levels of the cortical hierarchy in the TD group, whereas it was absent in the lower level of the hierarchy in the ASD group.

4.1. Intact detection of Gaborized objects in adolescents with ASD

TD and ASD adolescents were able to efficiently detect objects depicted by contour and/or texture (over 90% of correct detection). Accuracy and response times were not different between groups or conditions. Detecting such patterns requires the ability to perceptually group Gabor elements based on Gestalt properties. Indeed, disjoint local elements need to be grouped based on their orientations in order to delineate a shape and to segregate it from the noisy background. Note that the properties contributing to object identification in Gaborized object outlines have been carefully described in TD participants (see Panis and Wagemans, 2009; Torfs et al., 2010). Here, the absence of group differences suggests intact perceptual grouping abilities in adolescents with ASD, consistent with other studies reporting no evidence of impaired perceptual grouping in ASD (Blake et al., 2003; Del Viva et al., 2006; see Simmons et al., 2009 for a review; Dehaqani et al., 2016 for edge-defined objects; Van der Hallen et al., 2018). Conversely, decreased Gestalt perception in ASD, suggested by other studies (Bölte et al., 2007; Brosnan et al., 2004; Farran and Brosnan, 2011; Fitch et al., 2015; Jachim et al., 2015), would have predicted decreased performance in the ASD group, which was not observed in the present study. Hence, the behavioral results of this task do not provide support for theories describing decreased global processing in ASD (Happé and Frith, 2006; Mottron et al., 2006).

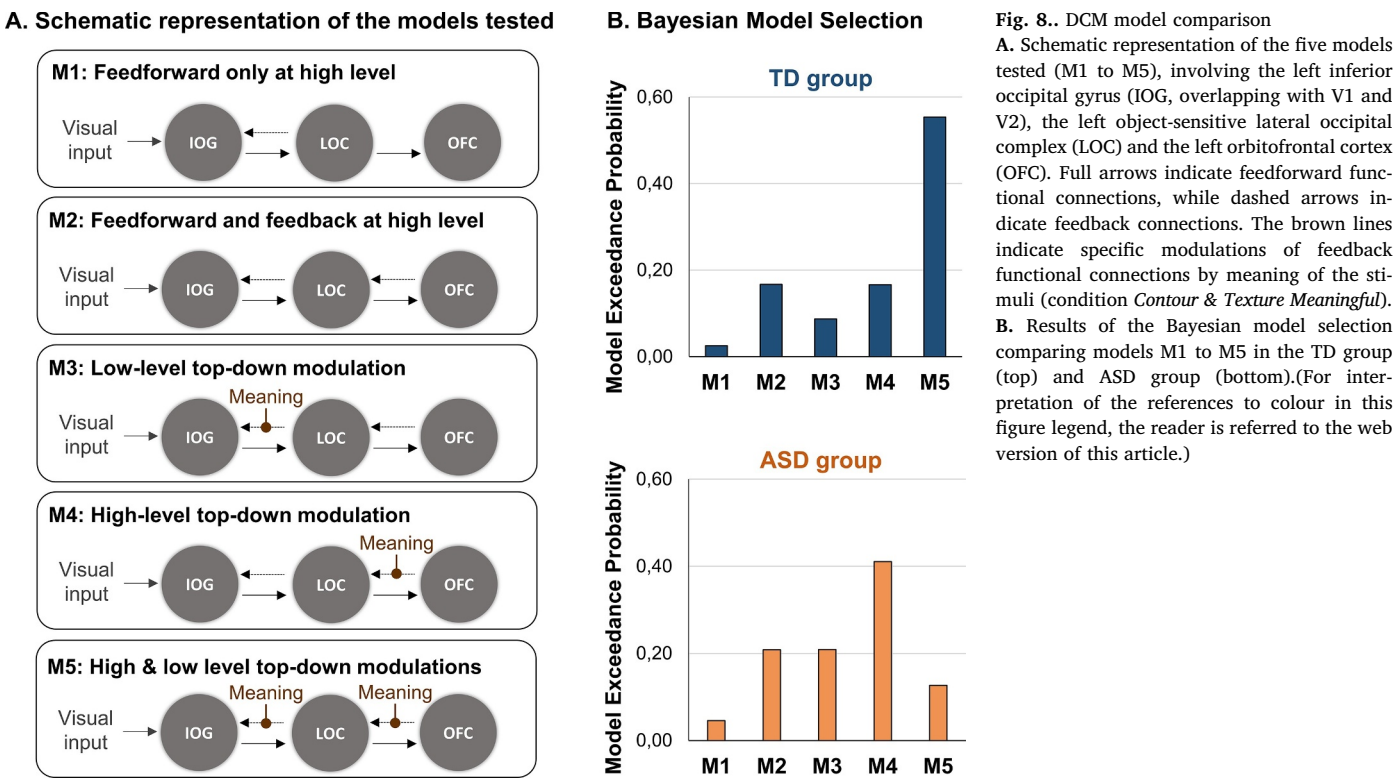

Fig. 8.. DCM model comparison
A. Schematic representation of the five models tested (M1 to M5), involving the left inferior occipital gyrus (IOG, overlapping with V1 and V2), the left object-sensitive lateral occipital complex (LOC) and the left orbitofrontal cortex (OFC). Full arrows indicate feedforward functional connections, while dashed arrows indicate feedback connections. The brown lines indicate specific modulations of feedback functional connections by meaning of the stimuli (condition *Contour & Texture Meaningful*). **B.** Results of the Bayesian model selection comparing models M1 to M5 in the TD group (top) and ASD group (bottom).(For interpretation of the references to colour in this figure legend, the reader is referred to the web version of this article.)

In another experiment using the *Contour & Texture Meaningful* stimuli (Evers et al., 2014), children and adolescents with ASD also had good accuracy levels to identify objects (above 90%). Yet, object identification was slower and less accurate in the ASD group than in the TD group (Evers et al., 2014). Contrary to the study by Evers and colleagues, participants involved in our experiment were not asked to explicitly identify the objects (and our participants were, on average, older). Yet, even though only shape detection was required in our study, perceptual grouping may have triggered top-down mechanisms contributing to object identification. Even for meaningless stimuli, a dynamic interplay between bottom-up and top-down processes may have contributed to match the Gaborized pattern to memorized object representations and to semantic knowledge.

4.2. Generally similar neural underpinnings of perceptual organization in ASD and TD adolescents

Occipitotemporal regions such as V1, V2, V3, V4 and the LOC, were activated during shape detection, consistently with the literature (Altmann et al., 2003; Cardin et al., 2011; Haxby et al., 2001; Ishai et al., 1999). Along the ventral visual stream hierarchy, these brain regions generally showed increased activity when stimuli were getting more and more organized and recognizable. Yet, at the lower level of the ventral stream hierarchy (V1/V2 cluster), the highest activity level was found for the random condition, and this activation level was significantly higher for random stimuli than for texture-defined patterns. In contrast, the LOC, playing a central role in object recognition (Gerlach et al., 2002; Grill-Spector et al., 1998; Haxby et al., 2001; Hayworth and Biederman, 2006; Malach et al., 1995), showed a strong increase in brain activity when stimuli were getting organized and meaningful. Note that previous studies also reported decreased activity in V1 associated with increased activity in the LOC for coherent shapes (Fang et al., 2008), as feedback from higher level regions would reduce the amplitude of neural activity at the lower levels of the hierarchy during perceptual grouping to facilitate object recognition (Fang et al., 2008; Hupé et al., 1998). Indeed, prior expectations (e.g., line orientations or object representations) reduce brain activity levels in V1, which contributes to sharpen representations in the early visual cortex and so, to interpret ambiguous visual stimuli (Kok et al., 2012).

In addition to the regions listed above and belonging to the ventral visual stream, other brain regions such as the hippocampus or the inferior frontal gyrus showed increased activation levels when stimuli were more organized. These two regions, together with the LOC, were also more activated when stimuli were recognizable objects than when stimuli were meaningless shapes. Interestingly, the hippocampus and the inferior frontal gyrus are associated with prior knowledge, memory and semantics (Adams and Janata, 2002; Gerlach et al., 1999; Sherman et al., 2016; Vuilleumier et al., 2002). The IFG would be involved in the integration of object representation with concepts in semantic memory across several sensory modalities (Adams and Janata, 2002). In addition, presenting meaningful stimuli may have been associated with silent labelling of the items by the participants. Such processes could explain the activity observed in the left IFG in both groups. As participants only needed to detect a shape and not to identify the objects, the verbal inputs from the left IFG may have been less critical than in a task where they would have needed to name the objects. In the contrast *Contour & Texture Meaningful* vs. *Meaningless*, the ASD group showed greater activation in the right IFG than the TD group (Fig. 6). Note that this could be related to an increased right-ward lateralization for ASD in language-specific tasks (Haesen et al., 2011; Herringshaw et al., 2016; Nielsen et al., 2014). Besides, during object recognition, the parahippocampal cortex may activate visual representations in the inferior temporal cortex (Bar, 2004). Meaningful stimuli also triggered increased activation in the orbitofrontal cortex in both groups. This region would store prior knowledge about visual object representations, helping to identify objects (Bar, 2004; Bar et al., 2006). The involvement of this brain region may have contributed to the identification of meaningful objects both in TD and ASD participants, even if the task simply consisted in detecting organized patterns. It also suggests that this high-level area sends top-down signals to facilitate object recognition, a process that would happen at the earlier

stages of visual processing (Bar et al., 2006; Fenske et al., 2006; Humphreys et al., 1997).

During object detection, the presence of facilitating top-down processes was suggested by the decreased activation in V1, increased activation in the LOC and increased involvement of frontal regions, but also by the connectivity results. Indeed, the functional connectivity patterns revealed increased network complexity characterized by more functional connections between frontal (IFG and OFC) and occipital regions when stimuli were getting more organized and recognizable. Furthermore, dynamic causal modelling results showed that in both groups, the best models encompassed both bottom-up and top-down functional connections between frontal and occipital regions. More precisely, in each group, feedforward and feedback functional connections were identified between three levels of the hierarchy: the OFC as a high-level region, the LOC as a mid-level region, and the inferior occipital gyrus as a low-level region. As previously mentioned, the LOC plays a fundamental role in object recognition, is involved in higher-level integration than the inferior occipital gyrus and would receive structural knowledge about objects (Gerlach et al., 2002). These results highlight the fact that the ventral visual stream is bidirectional and involves interactive bottom-up and top-down processes, facilitating perceptual grouping and object detection (Ahissar and Hochstein, 2004; Clark, 2013; Van Essen et al., 1992; Volberg and Greenlee, 2014), both in TD and ASD adolescents.

Consistently with the study by Humphreys and colleagues, we found that overall, the neural correlates of object perception were relatively similar in the TD and ASD groups and that the ASD group showed more activation variability in object-related brain areas than the TD group (Humphreys et al., 2008).

4.3. Reduced top-down processing in ASD during object detection?

Despite generally similar neural underpinnings in the TD and ASD groups, some group differences may indicate decreased top-down processing in the ASD group. Indeed, detecting meaningful objects (compared to baseline) was associated with a stronger activation in the LOC and middle occipital gyri in the ASD group than in the TD group. In line with the hypothesis of top-down signals explaining away sensory signals by decreasing the activation amplitude in lower-level regions (Kok et al., 2012), these greater activation levels in low and mid-level areas could be interpreted as a consequence of less top-down influence in the ASD group than in the TD group. Yet, note that the contrast between *Meaningful* and *Meaningless* stimuli was associated with an increased activation level in the right IFG and in the bilateral LOC in adolescents with ASD than in TD adolescents. While an increased activation level in these regions may seem contradictory with the hypothesis of decreased top-down processing in the ASD group, the increased activity level may not necessarily result in increased feedback from these regions.

In addition, despite no significant group differences in functional connectivity, we can notice that the number of functional connections between occipital and frontal regions tended to increase more clearly in the TD group than in the ASD group, when stimuli were getting more organized and meaningful. The networks of functional connections did not differ significantly between groups, but the strengths of these connections were differentially modulated by meaningful stimuli.

Indeed, the effective connectivity analyses revealed that top-down functional connections at the lower level of the hierarchy were not modulated by meaning in the ASD group, contrary to the TD group. Indeed, organized patterns that were recognizable led to a modulation of top-down functional connections from the OFC to the LOC and from the LOC to the inferior occipital gyrus in the TD group, whereas only the functional connections from the OFC to the LOC were modulated in the ASD group. We can hypothesize that in the meaningful condition, ASD participants applied less prior knowledge, which was associated with less functional connections between frontal and occipital regions, less modulation of top-down functional connections, and increased activation at the lower levels of the ventral visual stream hierarchy. These fMRI results would be in favor of theories suggesting that perception in ASD may be characterized by a reduced influence of prior knowledge in certain contexts (Pellicano and Burr, 2012).

Note that the group differences in neural correlates described above were not associated with decreased performance in the ASD group to detect shapes, but they may be related to increased difficulties in identifying objects, as evidenced in a previous study (Evers et al., 2014).

4.4. Limitations

One of the main limitations of this study is the relatively small sample size of each group.

Besides, using fMRI allowed us to precisely identify the brain regions involved in perceptual organization, but could not provide precise temporal information about this process. Using electrophysiological methods would be more suitable to study the temporal dynamics of perceptual grouping (Mijović et al., 2014) and to perform effective connectivity analyses (such as DCM analyses). Indeed, the results of the DCM analyses should be interpreted carefully, given the poor temporal resolution of fMRI data. In addition, it is important to keep in mind that the DCM analyses tested which of the five models best explained the data, but these models are of course a simplification of the actual neural mechanisms, and some other models (not tested here) could always exist that may better explain the data. Only a limited number of ROIs were chosen in the DCM analyses. As we restricted the set of ROIs to consider in these analyses, it is not unconceivable that additional results could have been obtained and different conclusions could have been formulated if we had chosen another set of brain regions.

Finally, we can highlight that the ASD group showed more variability in brain signal than the TD group. This increased variance may have reduced the sensitivity to detect group differences. Note that increased inter and intra variability of neural signal has been described in ASD (e.g., Milne, 2011; Poulin-Lord et al., 2014).

4.5. Conclusion

The ability to perceptually group local elements based on contour and/or texture, to perceive elements as a whole is preserved in adolescents with ASD. The ventral visual stream involved in this process was identified in TD and ASD adolescents and revealed only few group differences. When recognizable objects were presented, ASD participants may receive less top-down knowledge from high-level brain regions than TD participants. This may lead to less facilitation and to more difficulties identifying objects. In conclusion, the neural correlates of perceptual organization are preserved in ASD and allow global processing, but may be characterized by less top-down influence for recognizable objects.

Acronyms

ASD: Autism Spectrum Disorder, DCM: Dynamic Causal Modelling, GLM: General Linear Model, IFG: Inferior Frontal Gyrus, LOC: Lateral Occipital Complex, MRI: Magnetic Resonance Imaging, OFC: Orbitofrontal Cortex, ROI: Region Of Interest, TD: Typically Developing.

Funding

LAST was supported by a postdoctoral fellowship of the M.M. Delacroix Foundation. BB was supported by a postdoctoral fellowship of the Research Foundation Flanders and a visiting researcher grant of Fulbright. LVE was supported by a doctoral fellowship of the Research Foundation Flanders and a postdoctoral fellowship of the M.M.

Delacroix Foundation. The research was financed by grants from the Research Council of KU Leuven (IDO/08/013 and StG/15/014BF awarded to BB), an Excellence of Science grant (EOS: G0E8718N, HUMVISCAT) awarded to JW and BB, and a long-term structural funding from the Flemish Government (METH/14/02) to JW.

Declaration of Competing Interest

None

Acknowledgements

We thank all participating adolescents and their families for their time and effort. We also acknowledge Céline Gillebert (KU Leuven) and Patrick Dupont (UZ Leuven) for their support and discussion regarding the DCM analyses, Maarten Demeyer and Bart Machilsen for assistance creating the Gabor patterns, Farah Martens and Hans Op de Beeck (KU Leuven) for providing us with a functional mask of LOC, and Susan Whitfield-Gabrieli (MIT) for initial advise on using the ART Artifact Detection toolbox.

Supplementary materials

Supplementary material associated with this article can be found, in the online version, at doi:10.1016/j.nicl.2020.102197.

References

Adams, R.B., Janata, P., 2002. A comparison of neural circuits underlying auditory and visual object categorization. Neuroimage 16, 361–377. https://doi.org/10.1006/nimg.2002.1088.

Ahissar, M., Hochstein, S., 2004. The reverse hierarchy theory of visual perceptual learning. Trends Cogn. Sci. 8, 457–464. https://doi.org/10.1016/j.tics.2004.08.011.

Altmann, C.F., Bülthoff, H.H., Kourtzi, Z., 2003. Perceptual organization of local elements into global shapes in the human visual cortex. Curr. Biol. CB 13, 342–349.

American Psychiatric Association, 2000. Diagnostic and statistical manual of mental disorders, 4th ed.

Association, A.P., 2013. Diagnostic and Statistical Manual of Mental Disorders: Dsm-5, 5th Revised ed. American Psychiatric Publishing, Washington, DC.

Bar, M., 2007. The proactive brain: using analogies and associations to generate predictions. Trends Cogn. Sci. 11, 280–289. https://doi.org/10.1016/j.tics.2007.05.005.

Bar, M., 2004. Visual objects in context. Nat. Rev. Neurosci. 5, 617–629. https://doi.org/10.1038/nrn1476.

Bar, M., Kassam, K.S., Ghuman, A.S., Boshyan, J., Schmid, A.M., Dale, A.M., Hamalainen, M.S., Marinkovic, K., Schacter, D.L., Rosen, B.R., Halgren, E., 2006. Top-down facilitation of visual recognition. Proc. Natl. Acad. Sci. 103, 449–454. https://doi.org/10.1073/pnas.0507062103.

Behzadi, Y., Restom, K., Liau, J., Liu, T.T., 2007. A component based noise correction method (CompCor) for BOLD and perfusion based fMRI. Neuroimage 37, 90–101. https://doi.org/10.1016/j.neuroimage.2007.04.042.

Blake, R., Turner, L.M., Smoski, M.J., Pozdol, S.L., Stone, W.L., 2003. Visual recognition of biological motion is impaired in children with autism. Psychol. Sci. 14, 151–157. https://doi.org/10.1111/1467-9280.01434.

Spunt, B., 2016. spunt/bspmview: BSPMVIEW v.20161108. Zenodo. https://doi.org/10.5281/zenodo.168074.

Bölte, S., Holtmann, M., Poustka, F., Scheurich, A., Schmidt, L., 2007. Gestalt perception and local-global processing in high-functioning autism. J. Autism Dev. Disord. 37, 1493–1504. https://doi.org/10.1007/s10803-006-0231-x.

Brett, M., Anton, J.-L., Valabregue, R., Poline, J.-B., 2002. Region of interest analysis using an SPM toolbox. Present. 8th Int. Conf. Funct. Mapp. Hum. Brain June 2002, 2–6 Sendai Jpn.

Brock, J., 2012. Alternative bayesian accounts of autistic perception: comment on Pellicano and Burr. Trends Cogn. Sci. 16, 573–574. https://doi.org/10.1016/j.tics.2012.10.005.

Brosnan, M.J., Scott, F.J., Fox, S., Pye, J., 2004. Gestalt processing in autism: failure to process perceptual relationships and the implications for contextual understanding. J. Child Psychol. Psychiatry 45, 459–469.

Cardin, V., Friston, K.J., Zeki, S., 2011. Top-down modulations in the visual form pathway revealed with dynamic causal modeling. Cereb. Cortex N. Y. NY 21, 550–562. https://doi.org/10.1093/cercor/bhq122.

Casco, C., Campana, G., Han, S., Guzzon, D., 2009. Psychophysical and electrophysiological evidence of independent facilitation by collinearity and similarity in texture grouping and segmentation. Vision Res. 49, 583–593. https://doi.org/10.1016/j.visres.2009.02.004.

Chaumon, M., Kveraga, K., Barrett, L.F., Bar, M., 2014. Visual predictions in the orbitofrontal cortex rely on associative content. Cereb. Cortex 24, 2899–2907. https://doi.org/10.1093/cercor/bht146.

Clark, A., 2013. Whatever next? Predictive brains, situated agents, and the future of cognitive science. Behav. Brain Sci. 36, 181–204.

Critchley, H.D., Daly, E.M., Bullmore, E.T., Williams, S.C., Van Amelsvoort, T., Robertson, D.M., Rowe, A., Phillips, M., McAlonan, G., Howlin, P., Murphy, D.G., 2000. The functional neuroanatomy of social behaviour: changes in cerebral blood flow when people with autistic disorder process facial expressions. Brain J. Neurol. 123 (Pt 11), 2203–2212. https://doi.org/10.1093/brain/123.11.2203.

Dehaqani, M.-R.A., Zarei, M.A., Vahabie, A.-.H., Esteky, H., 2016. Impairment of perceptual closure in autism for vertex- but not edge-defined object images. J. Vis. 16, 10. https://doi.org/10.1167/16.10.10.

Del Viva, M.M., Igliozzi, R., Tancredi, R., Brizzolara, D., 2006. Spatial and motion integration in children with autism. Vision Res. 46, 1242–1252. https://doi.org/10.1016/j.visres.2005.10.018.

Demeyer, M., Machilsen, B., 2012. The construction of perceptual grouping displays using GERT. Behav. Res. Methods 44, 439–446. https://doi.org/10.3758/s13428-011-0167-8.

Eickhoff, S.B., Stephan, K.E., Mohlberg, H., Grefkes, C., Fink, G.R., Amunts, K., Zilles, K., 2005. A new SPM toolbox for combining probabilistic cytoarchitectonic maps and functional imaging data. Neuroimage 25, 1325–1335. https://doi.org/10.1016/j.neuroimage.2004.12.034.

Evers, K., Panis, S., Torfs, K., Steyaert, J., Noens, I., Wagemans, J., 2014. Disturbed interplay between mid- and high-level vision in ASD? Evidence from a contour identification task with everyday objects. J. Autism Dev. Disord. 44, 801–815. https://doi.org/10.1007/s10803-013-1931-7.

Fang, F., Kersten, D., Murray, S.O., 2008. Perceptual grouping and inverse fMRI activity patterns in human visual cortex. J. Vis. 8 (2), 1–9. https://doi.org/10.1167/8.7.2.

Farran, E.K., Brosnan, M.J., 2011. Perceptual grouping abilities in individuals with autism spectrum disorder; exploring patterns of ability in relation to grouping type and levels of development. Autism Res. Off. J. Int. Soc. Autism Res. 4, 283–292. https://doi.org/10.1002/aur.202.

Fenske, M.J., Aminoff, E., Gronau, N., Bar, M., 2006. Top-down facilitation of visual object recognition: object-based and context-based contributions. Prog. Brain Res. 155, 3–21. https://doi.org/10.1016/S0079-6123(06)55001-0.

Fitch, A., Fein, D.A., Eigsti, I.-.M., 2015. Detail and gestalt focus in individuals with optimal outcomes from autism spectrum disorders. J. Autism Dev. Disord. 45, 1887–1896. https://doi.org/10.1007/s10803-014-2347-8.

Friston, K., 2003. Learning and inference in the brain. Neural Netw. Off. J. Int. Neural Netw. Soc. 16, 1325–1352. https://doi.org/10.1016/j.neunet.2003.06.005.

Friston, K.J., Harrison, L., Penny, W., 2003. Dynamic causal modelling. Neuroimage 19, 1273–1302.

Frith, U., 1989. Autism: Explaining the Enigma. Oxford, UKCambridge, MA.

Gerlach, C., Aaside, C.T., Humphreys, G.W., Gade, A., Paulson, O.B., Law, I., 2002. Brain activity related to integrative processes in visual object recognition: bottom-up integration and the modulatory influence of stored knowledge. Neuropsychologia 40, 1254–1267.

Gerlach, C., Law, I., Gade, A., Paulson, O.B., 1999. Perceptual differentiation and category effects in normal object recognition: a PET study. Brain J. Neurol. 122 (Pt 11), 2159–2170.

Grill-Spector, K., Kushnir, T., Hendler, T., Edelman, S., Itzchak, Y., Malach, R., 1998. A sequence of object-processing stages revealed by fMRI in the human occipital lobe. Hum. Brain Mapp. 6, 316–328.

Grill-Spector, K., Weiner, K.S., 2014. The functional architecture of the ventral temporal cortex and its role in categorization. Nat. Rev. Neurosci. 15, 536–548. https://doi.org/10.1038/nrn3747.

Hadjikhani, N., Chabris, C.F., Joseph, R.M., Clark, J., McGrath, L., Aharon, I., Feczko, E., Tager-Flusberg, H., Harris, G.J., 2004. Early visual cortex organization in autism: an fMRI study. Neuroreport 15, 267–270. https://doi.org/10.1097/00001756-200402090-00011.

Haesen, B., Boets, B., Wagemans, J., 2011. A review of behavioural and electrophysiological studies on auditory processing and speech perception in autism spectrum disorders. Res. Autism Spectr. Disord. 5, 701–714. https://doi.org/10.1016/j.rasd.2010.11.006.

Happé, F., Frith, U., 2006. The weak coherence account: detail-focused cognitive style in autism spectrum disorders. J. Autism Dev. Disord. 36, 5–25. https://doi.org/10.1007/s10803-005-0039-0.

Haxby, J.V., Gobbini, M.I., Furey, M.L., Ishai, A., Schouten, J.L., Pietrini, P., 2001. Distributed and overlapping representations of faces and objects in ventral temporal cortex. Science 293, 2425–2430. https://doi.org/10.1126/science.1063736.

Hayworth, K.J., Biederman, I., 2006. Neural evidence for intermediate representations in object recognition. Vision Res. 46, 4024–4031. https://doi.org/10.1016/j.visres.2006.07.015.

Herringshaw, A.J., Ammons, C.J., DeRamus, T.P., Kana, R.K., 2016. Hemispheric differences in language processing in autism spectrum disorders: a meta-analysis of neuroimaging studies. Autism Res. Off. J. Int. Soc. Autism Res. 9, 1046–1057. https://doi.org/10.1002/aur.1599.

Hubl, D., Bölte, S., Feineis-Matthews, S., Lanfermann, H., Federspiel, A., Strik, W., Poustka, F., Dierks, T., 2003. Functional imbalance of visual pathways indicates alternative face processing strategies in autism. Neurology 61, 1232–1237. https://doi.org/10.1212/01.wnl.0000091862.22033.1a.

Humphreys, G.W., Riddoch, M.J., Price, C.J., 1997. Top-down processes in object identification: evidence from experimental psychology, neuropsychology and functional anatomy. Philos. Trans. R. Soc. Lond. B. Biol. Sci. 352, 1275–1282. https://doi.org/10.1098/rstb.1997.0110.

Humphreys, K., Hasson, U., Avidan, G., Minshew, N., Behrmann, M., 2008. Cortical patterns of category-selective activation for faces, places and objects in adults with autism. Autism Res. Off. J. Int. Soc. Autism Res. 1, 52–63. https://doi.org/10.1002/

aur.1.
Hupé, J.M., James, A.C., Payne, B.R., Lomber, S.G., Girard, P., Bullier, J., 1998. Cortical feedback improves discrimination between figure and background by V1, V2 and V3 neurons. Nature 394, 784–787. https://doi.org/10.1038/29537.
Ishai, A., Ungerleider, L.G., Martin, A., Schouten, J.L., Haxby, J.V., 1999. Distributed representation of objects in the human ventral visual pathway. Proc. Natl. Acad. Sci. U. S. A. 96, 9379–9384.
Jachim, S., Warren, P.A., McLoughlin, N., Gowen, E., 2015. Collinear facilitation and contour integration in autism: evidence for atypical visual integration. Front. Hum. Neurosci. 9. https://doi.org/10.3389/fnhum.2015.00115.
James, T.W., Culham, J., Humphrey, G.K., Milner, A.D., Goodale, M.A., 2003. Ventral occipital lesions impair object recognition but not object-directed grasping: an fMRI study. Brain J. Neurol. 126, 2463–2475. https://doi.org/10.1093/brain/awg248.
Kim, J.G., Biederman, I., Lescroart, M.D., Hayworth, K.J., 2009. Adaptation to objects in the lateral occipital complex (LOC): shape or semantics? Vision Res. 49, 2297–2305. https://doi.org/10.1016/j.visres.2009.06.020.
Kok, P., Jehee, J.F.M., de Lange, F.P., 2012. Less is more: expectation sharpens representations in the primary visual cortex. Neuron 75, 265–270. https://doi.org/10.1016/j.neuron.2012.04.034.
Kveraga, K., Ghuman, A.S., Bar, M., 2007. Top-down predictions in the cognitive brain. Brain Cogn. 65, 145–168. https://doi.org/10.1016/j.bandc.2007.06.007.
Lawson, R.P., Rees, G., Friston, K.J., 2014. An aberrant precision account of autism. Front. Hum. Neurosci. 8, 302. https://doi.org/10.3389/fnhum.2014.00302.
Machilsen, B., Wagemans, J., 2011. Integration of contour and surface information in shape detection. Vision Res. 51, 179–186. https://doi.org/10.1016/j.visres.2010.11.005.
Malach, R., Reppas, J.B., Benson, R.R., Kwong, K.K., Jiang, H., Kennedy, W.A., Ledden, P.J., Brady, T.J., Rosen, B.R., Tootell, R.B., 1995. Object-related activity revealed by functional magnetic resonance imaging in human occipital cortex. Proc. Natl. Acad. Sci. U. S. A. 92, 8135–8139.
Malisza, K.L., Clancy, C., Shiloff, D., Foreman, D., Holden, J., Jones, C., Paulson, K., Summers, R., Yu, C.T., Chudley, A.E., 2011. Functional evaluation of hidden figures object analysis in children with autistic disorder. J. Autism Dev. Disord. 41, 13–22. https://doi.org/10.1007/s10803-010-1013-z.
Martens, F., Bulthé, J., van Vliet, C., Op de Beeck, H., 2018. Domain-general and domain-specific neural changes underlying visual expertise. Neuroimage 169, 80–93. https://doi.org/10.1016/j.neuroimage.2017.12.013.
Mijović, B., De Vos, M., Vanderperren, K., Machilsen, B., Sunaert, S., Van Huffel, S., Wagemans, J., 2014. The dynamics of contour integration: a simultaneous EEG–fMRI study. Neuroimage 88, 10–21. https://doi.org/10.1016/j.neuroimage.2013.11.032.
Milne, E., 2011. Increased intra-participant variability in children with autistic spectrum disorders: evidence from single-trial analysis of evoked EEG. Front. Psychol. 2. https://doi.org/10.3389/fpsyg.2011.00051.
Mottron, L., Burack, J., 2001. Enhanced perceptual functioning in the development of autism. In: Burack, Charman, Yirmiya, Zelazo (Eds.), The development of autism: Perspectives from theory and research., in: The Development of Autism: Perspectives from Theory and Research. Erlbaum, Mahwah, NJ. pp. 131–148.
Mottron, L., Dawson, M., Soulières, I., Hubert, B., Burack, J., 2006. Enhanced perceptual functioning in autism: an update, and eight principles of autistic perception. J. Autism Dev. Disord. 36, 27–43. https://doi.org/10.1007/s10803-005-0040-7.
Mulder, M.J., Wagenmakers, E.-J., Ratcliff, R., Boekel, W., Forstmann, B.U., 2012. Bias in the brain: a diffusion model analysis of prior probability and potential payoff. J. Neurosci. Off. J. Soc. Neurosci. 32, 2335–2343. https://doi.org/10.1523/JNEUROSCI.4156-11.2012.
Murray, S.O., Kersten, D., Olshausen, B.A., Schrater, P., Woods, D.L., 2002. Shape perception reduces activity in human primary visual cortex. Proc. Natl. Acad. Sci. U. S. A. 99, 15164–15169. https://doi.org/10.1073/pnas.192579399.
Nielsen, J.A., Zielinski, B.A., Fletcher, P.T., Alexander, A.L., Lange, N., Bigler, E.D., Lainhart, J.E., Anderson, J.S., 2014. Abnormal lateralization of functional connectivity between language and default mode regions in autism. Mol. Autism 5, 8. https://doi.org/10.1186/2040-2392-5-8.
Panis, S., Wagemans, J., 2009. Time-course contingencies in perceptual organization and identification of fragmented object outlines. J. Exp. Psychol. Hum. Percept. Perform. 35, 661–687. https://doi.org/10.1037/a0013547.
Pei, F., Baldassi, S., Procida, G., Igliozzi, R., Tancredi, R., Muratori, F., Cioni, G., 2009. Neural correlates of texture and contour integration in children with autism spectrum disorders. Vision Res. 49, 2140–2150. https://doi.org/10.1016/j.visres.2009.06.006.
Pellicano, E., Burr, D., 2012. When the world becomes “too real”: a bayesian explanation of autistic perception. Trends Cogn. Sci. 16, 504–510. https://doi.org/10.1016/j.tics.2012.08.009.
Pierce, K., Müller, R.A., Ambrose, J., Allen, G., Courchesne, E., 2001. Face processing occurs outside the fusiform “face area” in autism: evidence from functional MRI. Brain J. Neurol. 124, 2059–2073.
Poulin-Lord, M.-P., Barbeau, E.B., Soulières, I., Monchi, O., Doyon, J., Benali, H., Mottron, L., 2014. Increased topographical variability of task-related activation in perceptive and motor associative regions in adult autistics. NeuroImage Clin. 4, 444–453. https://doi.org/10.1016/j.nicl.2014.02.008.
Rao, R.P., Ballard, D.H., 1999. Predictive coding in the visual cortex: a functional interpretation of some extra-classical receptive-field effects. Nat. Neurosci. 2, 79–87. https://doi.org/10.1038/4580.
Ring, H.A., Baron-Cohen, S., Wheelwright, S., Williams, S.C.R., Brammer, M., Andrew, C., Bullmore, E.T., 1999. Cerebral correlates of preserved cognitive skills in autismA functional MRI study of embedded figures task performance. Brain 122, 1305–1315. https://doi.org/10.1093/brain/122.7.1305.
Roeyers, H., Thys, M., Druart, C., De Schryver, M., Schittekatte, M., 2013. Screeninglijst voor autismespectrumstoornissen: SRS-2. Amst. Hogrefe Uitgevers Bv.
Roeyers, H., Thys, M., Druart, C., De Schryver, M., Schittekatte, M., 2011. Screeninglijst voor autismespectrumstoornissen: SRS. Amst. Hogrefe Uitgevers Bv.
Sassi, M., Machilsen, B., Wagemans, J., 2012. Shape detection of Gaborized outline versions of everyday objects. Percept 3, 745–764. https://doi.org/10.1068/i0499.
Sassi, M., Vancleef, K., Machilsen, B., Panis, S., Wagemans, J., 2010. Identification of everyday objects on the basis of Gaborized outline versions. Percept 1, 121–142. https://doi.org/10.1068/i0384.
Scherf, K.S., Elbich, D., Minshew, N., Behrmann, M., 2014. Individual differences in symptom severity and behavior predict neural activation during face processing in adolescents with autism. NeuroImage Clin. 7, 53–67. https://doi.org/10.1016/j.nicl.2014.11.003.
Scherf, K.S., Luna, B., Minshew, N., Behrmann, M., 2010. Location, location, location: alterations in the functional topography of face- but not object- or place-related cortex in adolescents with autism. Front. Hum. Neurosci. 4. https://doi.org/10.3389/fnhum.2010.00026.
Schultz, R.T., Gauthier, I., Klin, A., Fulbright, R.K., Anderson, A.W., Volkmar, F., Skudlarski, P., Lacadie, C., Cohen, D.J., Gore, J.C., 2000. Abnormal ventral temporal cortical activity during face discrimination among individuals with autism and Asperger syndrome. Arch. Gen. Psychiatry 57, 331–340. https://doi.org/10.1001/archpsyc.57.4.331.
Sewards, T.V., Sewards, M.A., 2002. On the neural correlates of object recognition awareness: relationship to computational activities and activities mediating perceptual awareness. Conscious. Cogn. 11, 51–77. https://doi.org/10.1006/ccog.2001.0518.
Sherman, M.T., Seth, A.K., Kanai, R., 2016. Predictions shape confidence in right inferior frontal gyrus. J. Neurosci. Off. J. Soc. Neurosci. 36, 10323–10336. https://doi.org/10.1523/JNEUROSCI.1092-16.2016.
Skuse, D., Warrington, R., Bishop, D., Chowdhury, U., Lau, J., Mandy, W., Place, M., 2004. The developmental, dimensional and diagnostic interview (3di): a novel computerized assessment for autism spectrum disorders. J. Am. Acad. Child Adolesc. Psychiatry 43, 548–558. https://doi.org/10.1097/00004583-200405000-00008.
Snodgrass, J.G., Vanderwart, M., 1980. A standardized set of 260 pictures: norms for name agreement, image agreement, familiarity, and visual complexity. J. Exp. Psychol. [Hum. Learn.] 6, 174–215.
Torfs, K., Panis, S., Wagemans, J., 2010. Identification of fragmented object outlines: a dynamic interplay between different component processes. Vis. Cogn. 18, 1133–1164. https://doi.org/10.1080/13506281003693593.
Van de Cruys, S., Evers, K., Van der Hallen, R., Van Eylen, L., Boets, B., de-Wit, L., Wagemans, J., 2014. Precise minds in uncertain worlds: predictive coding in autism. Psychol. Rev. 121, 649–675. https://doi.org/10.1037/a0037665.
Van der Hallen, R., Evers, K., Brewaeys, K., Van den Noortgate, W., Wagemans, J., 2015. Global processing takes time: a meta-analysis on local-global visual processing in asd. Psychol. Bull. 141, 549–573. https://doi.org/10.1037/bul0000004.
Van der Hallen, R., Evers, K., de-Wit, L., Steyaert, J., Noens, I., Wagemans, J., 2018. Multiple object tracking reveals object-based grouping interference in children with ASD. J. Autism Dev. Disord. 48, 1341–1349. https://doi.org/10.1007/s10803-015-2463-0.
Van Essen, D.C., Anderson, C.H., Felleman, D.J., 1992. Information processing in the primate visual system: an integrated systems perspective. Science 255, 419–423.
Vinberg, J., Grill-Spector, K., 2008. Representation of shapes, edges, and surfaces across multiple cues in the human visual cortex. J. Neurophysiol. 99, 1380–1393. https://doi.org/10.1152/jn.01223.2007.
Volberg, G., Greenlee, M.W., 2014. Brain networks supporting perceptual grouping and contour selection. Front. Psychol. 5, 264. https://doi.org/10.3389/fpsyg.2014.00264.
Vuilleumier, P., Henson, R.N., Driver, J., Dolan, R.J., 2002. Multiple levels of visual object constancy revealed by event-related fMRI of repetition priming. Nat. Neurosci. 5, 491–499. https://doi.org/10.1038/nn839.
Wager, T.D., Nichols, T.E., 2003. Optimization of experimental design in fMRI: a general framework using a genetic algorithm. Neuroimage 18, 293–309.
Walter, B., Blecker, C., Kirsch, P., Sammer, G., Stark, R., Vaitl, D., 2003. MARINA: an easy to use tool for the creation of MAsks for Region of INterest Analyses [abstract]. In: Presented at the 9th International Conference on Functional Mapping of the Human Brain. 19 Available CD-Rom NeuroImage.
Whitfield-Gabrieli, S., Nieto-Castanon, A., 2012. Conn: a functional connectivity toolbox for correlated and anticorrelated brain networks. Brain Connect. 2, 125–141. https://doi.org/10.1089/brain.2012.0073.
Wilson, H.R., Wilkinson, F., 2015. From orientations to objects: configural processing in the ventral stream. J. Vis. 15, 4. https://doi.org/10.1167/15.7.4.